
Background Modeling via Uncertainty Estimation for Weakly-supervised Action Localization

Pilhyeon Lee^{1*} Jinglu Wang² Yan Lu² Hyeran Byun^{1†}

¹Yonsei University ²Microsoft Research

{lph1114, hrbyun}@yonsei.ac.kr {jinglwa, yanlu}@microsoft.com

Abstract

Weakly-supervised temporal action localization aims to detect intervals of action instances with only video-level action labels for training. A crucial challenge is to separate frames of action classes from remaining, denoted as background frames (*i.e.*, frames not belonging to any action class). Previous methods attempt background modeling by either synthesizing pseudo background videos with static frames or introducing an auxiliary class for background. However, they overlook an essential fact that background frames could be dynamic and inconsistent. Accordingly, we cast the problem of identifying background frames as out-of-distribution detection and isolate it from conventional action classification. Beyond our base action localization network, we propose a module to estimate the probability of being background (*i.e.*, *uncertainty* [20]), which allows us to learn uncertainty given only video-level labels via multiple instance learning. A background entropy loss is further designed to reject background frames by forcing them to have uniform probability distribution for action classes. Extensive experiments verify the effectiveness of our background modeling and show that our method significantly outperforms state-of-the-art methods on the standard benchmarks - THUMOS'14 and ActivityNet (1.2 and 1.3). Our code and the trained model are available at <https://github.com/Pilhyeon/Background-Modeling-via-Uncertainty-Estimation>.

1 Introduction

Temporal action localization (TAL) is a very challenging problem of finding and classifying action intervals in untrimmed videos, which plays a crucial role in video understanding and analysis. Due to its wide applications (*e.g.*, video surveillance [42], video summarization [22, 45], action retrieval [28]), TAL has drawn much attention from the research community. A lot of work has been done in the fully-supervised manner and achieved impressive progress [37, 38, 47, 57, 9, 24, 27, 25, 55]. However, they suffer from the extremely high cost of acquiring precise temporal annotations.

To relieve the high-cost issue and enlarge the scalability, researchers direct their attention to the same task with weak supervision, namely weakly-supervised temporal action localization (WTAL). Among the various levels of weak supervision, thanks to the cheap cost, video-level action label is mainly utilized [43, 40, 39], while other types (*e.g.*, temporal ordering [5, 19, 16], frequencies of action instances [49, 33]) are also explored. In this paper, we follow the mainstream using only video-level labels, where each video is labeled as positive for action classes if it contains corresponding action frames and as negative otherwise. Note that a video may have multiple action classes as its label.

Existing work adopts attention mechanism [34, 54] or multiple instance learning formulation [36, 33] to predict frame-level class scores from video-level labels. Nonetheless, weakly-supervised methods

*This work was done while he was a research intern at Microsoft Research.

†Corresponding author

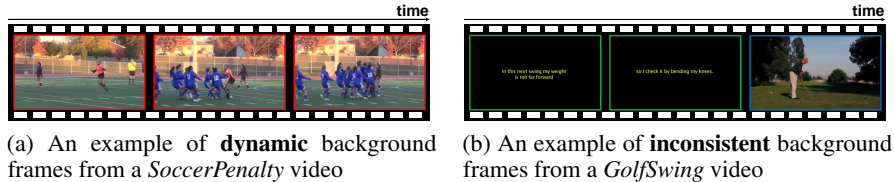


Figure 1: Observation on dynamism and inconsistency of background frames from THUMOS’14. It should be noted that none of them contain any action instance, *i.e.*, they are all background frames. (a) The frames in the red box showing soccer players celebrating are very dynamic, even though they are background frames. (b) There are two types of background frames: black scenes with subtitles (green box) and a golfer preparing to shoot (blue box). These two types have very inconsistent appearances.

still show highly inferior performances when compared to fully-supervised ones. According to the recent literature [49, 26, 35, 21], the performance degradation comes from the false alarms of complex background frames, since video-level labels do not have any clue for background. To bridge the gap, some studies [26, 35, 21] attempt background modeling in the weakly-supervised setting. Liu *et al.* [26] synthesize pseudo background videos by merging static frames and label them as the background class, assuming all background frames are static. However, the assumption is too strong and cannot cover all scenarios, as some background frames could be dynamic (Fig. 1a). Nguyen *et al.* [35] and BaS-Net [21] observe that every untrimmed video has background frames, and identify such background frames as the background class. Still, it is difficult to force all background frames to belong to one specific class, as they may have very inconsistent appearances or semantics (Fig. 1b).

In this paper, we embrace the observation on dynamism and inconsistency in background frames, and propose to formulate the problem of rejecting background frames as out-of-distribution detection problem [15, 23], where action and background are mapped to in-distribution and out-of-distribution, respectively. To detect out-of-distribution samples, it is natural to estimate the probability that a sample is from out-of-distribution, also known as *uncertainty* [4, 20, 11]. Accordingly, we aim to estimate uncertainty (*i.e.*, the probability of being background) to identify background frames. Regarding that background frames should have low scores for all action classes, we utilize feature magnitudes to model uncertainty, *i.e.*, our model needs to produce feature vectors with large magnitudes for action frames while ones with small magnitudes for background frames. Unfortunately, it is inappropriate to directly handle individual frames, as we do not have frame-level labels in weakly-supervised setting.

In order to learn uncertainty only with video-level supervision, we leverage the formulation of multiple instance learning [32, 2, 58], where a model is trained with a bag (*i.e.*, untrimmed video) instead of instances (*i.e.*, frames). From each untrimmed video, we select top-k and bottom-k frames in terms of the feature magnitude and consider them as pseudo action and background frames, respectively. Thereafter, we design uncertainty modeling loss to manipulate the magnitudes of pseudo action/background features, which enables our model to learn uncertainty without frame-level labels. Moreover, we introduce background entropy loss to force pseudo background frames to have uniform probability distribution for action classes. By jointly optimizing the losses for background modeling along with a general action classification loss, our model successfully separates action frames from background frames, achieving a new state-of-the-art performance with a large margin on THUMOS’14 and ActivityNet. The effectiveness of our method is verified by ablation study.

Summary of contributions. Our contributions are three-fold: 1) We are the first to formulate background frames as out-of-distribution, overcoming the difficulty in modeling background with regard to their unconstrained and inconsistent properties. 2) We design a new framework for weakly-supervised action localization, where uncertainty is learned for background modeling only with video-level labels via multiple instance learning. 3) We further encourage separation between action and background with a loss maximizing the entropy of action probability distribution from background frames.

2 Related Work

Fully-supervised action localization. The goal of temporal action localization is to find temporal intervals of action instances from long untrimmed videos and classify them. For the task, many

approaches depend on accurate temporal annotations for each training video, *i.e.*, start time and end time of action instances. Most of them first generate proposals, and then classify them. To generate proposals, some methods adopt sliding window method [37, 53, 38, 50, 46, 9], while others predict start and end frames of action instances [24, 25]. Moreover, there are gaussian modeling of each action instance [27] and an efficient method without proposal generation [1]. It should be noted that fully-supervised methods leverage frame-level annotations to distinguish action and background frames, while weakly-supervised ones do not.

Weakly-supervised action localization. Recently, due to the extremely high cost of frame-wise annotations, many attempts have been made to solve temporal action localization with weak supervision, mostly video-level labels. UntrimmedNets [43] first tackle the problem by selecting relevant segments on soft and hard ways. STPN [34] forces the model to select sparse action segments, while Hide-and-peek [40] and MAAN [54] extend discriminative parts by randomly hiding or sampling segments, respectively. W-TALC [36] and 3C-Net [33] both employ deep metric learning to force features from the same action to get closer to themselves than those from different action classes. Meanwhile, AutoLoc [39] and CleanNet [51] attempt to regress the intervals of action instances, instead of performing hard thresholding. TSM [52] proposes to model each action instance as a multi-phase process and predict the evolving sequence of phases. There are also several studies exploiting additional information, *e.g.*, the frequency of action instances [49, 33], human pose [56].

Apart from the methods above, Liu *et al.* [26], Nguyen *et al.* [35] and BaS-Net [21] are the ones to seek to explicitly model background. However, as mentioned in Sec. 1, they have innate limitations in that background frames could be dynamic and inconsistent, which leads to difficulty in separating background. On the other hand, we consider background as out-of-distribution regarding its properties and propose to learn uncertainty as well as action class scores. In experiments, the effectiveness of our approach is verified, while outperforming the state-of-the-art methods by a large margin.

Out-of-distribution detection. The aim of out-of-distribution detection is to determine whether an input sample comes from in-distribution (*i.e.*, training distribution) or not [15, 23, 11]. The problem has also been studied in several different ways such as open-set recognition [3, 4], outlier rejection [48, 13], anomaly detection [8], or uncertainty estimation [14, 12, 41, 20, 29–31]. To tackle the problem, ODIN [23] uses temperature scaling in the softmax function and adds small perturbations to the input. Meanwhile, Lakshminarayanan *et al.* [20] and Dhamija *et al.* [11] predict uncertainty of samples by using the MLP ensemble model and the feature magnitudes, respectively. Moreover, OpenMax [4] directly estimates uncertainty without using any out-of-distribution sample for training.

3 Method

In this section, we provide the details of the proposed method. The overview of our architecture is illustrated in Fig. 2. We first set up our baseline with the conventional pipeline for weakly-supervised action localization (Sec. 3.1). Next, we cast background identification problem as out-of-distribution detection and tackle it by modeling uncertainty (Sec. 3.2). Thereafter, the objective functions to train our model are introduced (Sec. 3.3). Lastly, we explain how the inference is performed (Sec. 3.4).

3.1 Main pipeline

Feature extraction. Due to the memory constraint, we first split each video into multi-frame non-overlapping segments, $v_n = \{s_{n,l}\}_{l=1}^{L_n}$, where L_n denotes the number of segments in the n -th video v_n . To handle the large variation in video lengths, a fixed number of T segments $\{\tilde{s}_{n,t}\}_{t=1}^T$ are sampled from each original video. Then spatio-temporal features $x_{n,t}^{\text{RGB}} \in \mathbb{R}^D$ and $x_{n,t}^{\text{flow}} \in \mathbb{R}^D$ are extracted from the sampled RGB and flow segments, respectively. Note that any feature extractor can be used. Afterwards, we concatenate the RGB and flow features into complete feature vectors $x_{n,t} \in \mathbb{R}^{2D}$, which are then stacked to build a feature map of length T , *i.e.*, $X_n = [x_{n,1}, \dots, x_{n,T}] \in \mathbb{R}^{2D \times T}$.

Feature embedding. To embed the extracted features, we feed them into a single 1-D convolutional layer followed by ReLU activation. Formally, $F_n = g_{\text{embed}}(X_n; \phi_{\text{embed}})$, where g_{embed} denotes the convolution operator with the activation function and ϕ_{embed} is the learnable parameters of the convolutional layer. Concretely, the dimension of the embedded features is the same as that of input features, *i.e.*, $F_n = [f_{n,1}, \dots, f_{n,T}] \in \mathbb{R}^{2D \times T}$.

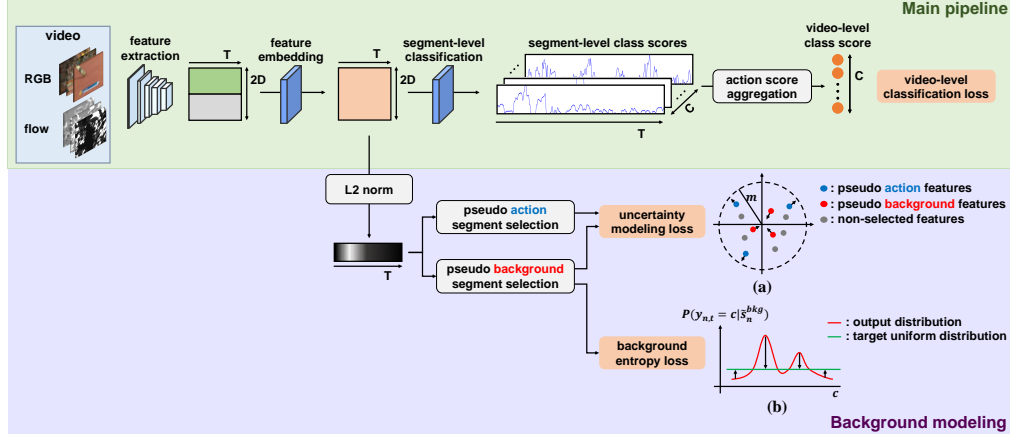


Figure 2: Overview of the proposed method. The main pipeline serves the conventional process for weakly-supervised action localization. In the background modeling part, the pseudo action/background segments are selected based on features magnitudes, which are used to calculate two losses for background modeling: (a) uncertainty modeling loss which enlarges and reduces the feature magnitudes of the pseudo action and background segments respectively, and (b) background entropy loss forcing the pseudo background segments to have uniform action probability distribution.

Segment-level classification. From the embedded features, we predict segment-level class scores, which are later used for action localization. For the n -th video v_n , the class scores are derived by the action classifier, *i.e.*, $\mathcal{A}_n = g_{\text{cls}}(F_n; \phi_{\text{cls}})$, where g_{cls} represents the linear classifier with parameters ϕ_{cls} , $\mathcal{A}_n \in \mathbb{R}^{C \times T}$ denotes the segment-level action scores, and C is the number of action classes.

Action score aggregation. Adopting multiple instance learning [32, 2, 58], we aggregate top k^{act} scores along all segments for each action class and average them to build a video-level class score:

$$a_c(v_n) = \frac{1}{k^{\text{act}}} \max_{\substack{\hat{\mathcal{A}}_{n;c} \subset \mathcal{A}_n[c,:], \\ |\hat{\mathcal{A}}_{n;c}| = k^{\text{act}}}} \sum_{a \in \hat{\mathcal{A}}_{n;c}} a, \quad (1)$$

where $\hat{\mathcal{A}}_{n;c}$ is the subset containing k^{act} action scores for class c , and k^{act} is a hyper-parameter controlling the number of the aggregated segments.

Thereafter, we obtain the video-level action probability for each action class by applying the softmax function to the aggregated scores:

$$p_c(v_n) = \frac{\exp(a_c(v_n))}{\sum_{c'=1}^C \exp(a_{c'}(v_n))}, \quad (2)$$

where $p_c(v_n)$ represents the softmax score for c -th action of n -th video.

3.2 Considering background as out-of-distribution

Decomposition of action localization. From the main pipeline, we obtain the action probabilities for each segment, but the essential component for action localization, *i.e.*, background identification, is not carefully considered. Regarding the unconstraint and inconsistency of background frames, we treat background as out-of-distribution [4, 20, 11]. Considering the probability for class c of segment $\tilde{s}_{n,t}$, it can be decomposed into two parts with the chain rule, *i.e.*, the in-distribution action classification and the background identification. Let $d \in \{0, 1\}$ denotes the variable for the background identification. If the segment belongs to any action class, let $d = 1$, otherwise $d = 0$ (belongs to background). Then, the posterior probability for class c of $\tilde{s}_{n,t}$ is given by:

$$\begin{aligned} P(y_{n,t} = c | \tilde{s}_{n,t}) &= P(y_{n,t} = c, d = 1 | \tilde{s}_{n,t}) \\ &= P(y_{n,t} = c | d = 1, \tilde{s}_{n,t}) P(d = 1 | \tilde{s}_{n,t}), \end{aligned} \quad (3)$$

where $y_{n,t}$ is the label of the corresponding segment, *i.e.*, if $\tilde{s}_{n,t}$ belongs to the c -th action class, then $y_{n,t} = c$, while $y_{n,t} = 0$ for background segments.

Uncertainty modeling. In Eq. 3, the probability for in-distribution action classification, *i.e.*, $P(y_{n,t} = c | d = 1, \tilde{s}_{n,t})$, is estimated with the softmax function as in general classification task. Additionally, it is necessary to model the probability that a segment belongs to any action class *i.e.*, $P(d = 1 | \tilde{s}_{n,t})$, to tackle background identification problem. Assuming that background frames should produce low scores for all action classes, we model uncertainty with the magnitudes of feature vectors, namely, background features have small magnitudes, while action features have large ones. Then the probability that the t -th segment in the n -th video ($\tilde{s}_{n,t}$) is an action segment is defined by:

$$P(d = 1 | \tilde{s}_{n,t}) = \frac{\min(m, \|f_{n,t}\|)}{m}, \quad (4)$$

where $f_{n,t}$ is the corresponding feature vector of $\tilde{s}_{n,t}$, $\|\cdot\|$ is a norm function (we use L-2 norm here), and m is the pre-defined maximum feature magnitude. From the equation, it is ensured that the probability falls between 0 and 1, *i.e.*, $0 \leq P(d = 1 | \tilde{s}_{n,t}) \leq 1$.

Multiple instance learning. To learn uncertainty only with video-level labels, we borrow the concept of multiple instance learning [32, 2, 58], where a model is trained with a bag (*i.e.*, untrimmed video), rather than instances (*i.e.*, segments). In this setting, we select the top k^{act} segments in terms of the feature magnitude, and treat them as the pseudo action segments $\{\tilde{s}_{n,i} | i \in \mathcal{S}^{\text{act}}\}$, where \mathcal{S}^{act} indicates the set of pseudo action indices. Meanwhile, the bottom k^{bkg} segments are considered as the pseudo background segments $\{\tilde{s}_{n,j} | j \in \mathcal{S}^{\text{bkg}}\}$, where \mathcal{S}^{bkg} denotes the set of indices for pseudo background. k^{act} and k^{bkg} represent the number of segments sampled for action and background, respectively. Then the pseudo action/background segments serve as the representatives of the input untrimmed video, and they are used for training the model with video-level labels.

3.3 Training objectives

Our model is optimized with three losses: 1) video-level classification loss \mathcal{L}_{cls} for action classification of each input video, 2) uncertainty modeling loss \mathcal{L}_{um} which manipulates the magnitudes of action and background feature vectors for background identification, and 3) background entropy loss \mathcal{L}_{be} for preventing background segments from having a high probability for any action class. The overall loss function is as follows:

$$\mathcal{L}_{\text{total}} = \mathcal{L}_{\text{cls}} + \alpha \mathcal{L}_{\text{um}} + \beta \mathcal{L}_{\text{be}}, \quad (5)$$

where α and β are hyper-parameters for balancing the losses.

Video-level classification loss. For multi-label action classification, we use the binary cross entropy loss with normalized video-level labels [43] as follows:

$$\mathcal{L}_{\text{cls}} = \frac{1}{N} \sum_{n=1}^N \sum_{c=1}^C -y_{n,c} \log p_c(v_n), \quad (6)$$

where $p_c(v_n)$ represents the video-level softmax score for the c -th class of the n -th video (Eq. 2), and $y_{n,c}$ is the normalized video-level label for the c -th class of the n -th video.

Uncertainty modeling loss. In order to learn uncertainty, we train the model to produce feature vectors with large magnitudes for pseudo action segments but ones with small magnitudes for pseudo background segments, as illustrated in Fig. 2 (a). Formally, uncertainty modeling loss takes the form:

$$\mathcal{L}_{\text{um}} = \frac{1}{N} \sum_{n=1}^N (\max(0, m - \|f_n^{\text{act}}\|) + \|f_n^{\text{bkg}}\|)^2, \quad (7)$$

where $f_n^{\text{act}} = \frac{1}{k^{\text{act}}} \sum_{i \in \mathcal{S}^{\text{act}}} f_{n,i}$ and $f_n^{\text{bkg}} = \frac{1}{k^{\text{bkg}}} \sum_{j \in \mathcal{S}^{\text{bkg}}} f_{n,j}$ are the mean features of the pseudo action and background segments of the n -th video, respectively. $\|\cdot\|$ is the norm function, and m is the pre-defined maximum feature magnitude, the same in Eq. 4.

Background entropy loss. Though uncertainty modeling loss encourages background segments to produce low scores for all actions, softmax scores for some action classes could be high due to the relativeness of softmax function. To prevent background segments from having a high softmax score

for any action class, we define a loss function which maximizes the entropy of action probabilities of background segments, *i.e.*, background segments are forced to have uniform probability distribution for action classes as described in Fig. 2 (b). Background entropy loss is calculated as follows:

$$\mathcal{L}_{\text{be}} = \frac{1}{NC} \sum_{n=1}^N \sum_{c=1}^C -\log(p_c(\tilde{s}_n^{\text{bkg}})), \quad (8)$$

where $p_c(\tilde{s}_n^{\text{bkg}}) = \frac{1}{k^{\text{bkg}}} \sum_{j \in \mathcal{S}^{\text{bkg}}} p_c(\tilde{s}_{n,j})$ is the averaged action probability for the c -th class of the pseudo background segments, and $p_c(\tilde{s}_{n,j})$ is the softmax score for the c -th class of the segment $\tilde{s}_{n,j}$.

3.4 Inference

At the test time, for an input video, we first obtain the video-level softmax score and threshold on it with θ_{vid} to determine which action classes are localized. For the remaining action classes, we calculate the segment-level posterior probability by multiplying the segment-level softmax score and the probability of being an action segment as in Eq. 3. Afterwards, the segments whose posterior probabilities are larger than θ_{seg} are selected as the candidate segments. Finally, consecutive candidate segments are grouped into a single proposal. Since we use multiple thresholds for θ_{seg} , non-maximum suppression (NMS) is performed for the proposals. We note that no duplicate proposal is allowed.

4 Experiments

4.1 Experimental settings

Datasets. THUMOS’14 [18] is a widely used dataset for temporal action localization, containing 200 validation videos and 213 test videos of 20 action classes. It is very challenging as the lengths of the videos are diverse and actions frequently occur (on average 15 instances per video). We use validation videos for training and test videos for test. On the other hand, ActivityNet [6] is a large-scale benchmark containing two versions (1.2 and 1.3). ActivityNet 1.3, consisting of 200 action categories, has 10,024 training videos, 4,926 validation videos and 5,044 test videos. ActivityNet 1.2 is a subset of the version 1.3, and is composed of 4,819 training videos, 2,383 validation videos and 2,480 test videos of 100 action classes. Because the ground-truths for the test videos of ActivityNet are withheld for the challenge, we utilize validation videos for evaluation.

Evaluation metrics. We evaluate our method with mean average precisions (mAPs) under several different intersection of union (IoU) thresholds, which are the standard evaluation metrics for temporal action localization. The official evaluation code of ActivityNet³ is used for measuring mAPs.

Implementation details. We employ two different feature extractors, namely UntrimmedNets [43] and I3D networks [7] pre-trained on ImageNet [10] and Kinetics [7], respectively. Each input segment consists of 5 frames for UntrimmedNets and 16 frames for I3D. It should be noted that we do not finetune the feature extractor for fair comparison. TVL1 algorithm [44] is used to extract optical flow from videos. We fix the number of segments T as 750 and 50 for THUMOS’14 and ActivityNet, respectively. The sampling method is the same as STPN [34]. The number of the pseudo action/background frames is determined by the ratio parameters, *i.e.*, $k^{\text{act}} = T/r^{\text{act}}$ and $k^{\text{bkg}} = T/r^{\text{bkg}}$. All hyper-parameters are set by grid search; $m = 100$, $r^{\text{act}} = 8$, $r^{\text{bkg}} = 6$, $\alpha = 10^{-4}$, $\beta = 1$, and $\theta_{\text{vid}} = 0.2$. To enrich the proposal pool, we use multiple thresholds from 0 to 0.25 with a step size 0.025 for θ_{seg} , then perform non-maximum suppression (NMS) with IoU threshold 0.7.

4.2 Comparison with state-of-the-art methods

We compare our method with the existing fully-supervised and weakly-supervised methods under several IoU thresholds. The results on THUMOS’14, ActivityNet 1.2, and 1.3 are reported in Table 1, Table 2, and Table 3, respectively. We separate the entries by horizontal lines regarding the levels of supervision. For readability, all results are reported on the percentage scale.

³<https://github.com/activitynet/ActivityNet/tree/master/Evaluation>

Table 1: Comparison on THUMOS’14. † indicates the use of additional information, such as action frequency or human pose. UNT and I3D denote the use of UntrimmedNets and I3D features respectively, while AVG represents the average mAP under the thresholds 0.3:0.1:0.7.

Supervision	Method	Feature	mAP@IoU (%)					AVG
			0.3	0.4	0.5	0.6	0.7	
Full	S-CNN [37]	-	36.3	28.7	19.0	10.3	5.3	19.9
	CDC [38]	-	40.1	29.4	23.3	13.1	7.9	22.8
	R-C3D [47]	-	44.8	35.6	28.9	-	-	-
	SSN [57]	-	51.9	41.0	29.8	-	-	-
	TAL-Net [9]	-	53.2	48.5	42.8	33.8	20.8	39.8
	BSN [24]	-	53.5	45.0	36.9	28.4	20.0	36.8
	GTAN [27]	-	57.8	47.2	38.8	-	-	-
	BMN [25]	-	56.0	47.4	38.8	29.7	20.5	38.5
	P-GCN [55]	-	63.6	57.8	49.1	-	-	-
Weak†	STAR [49]	I3D	48.7	34.7	23.0	-	-	-
	3C-Net [33]	I3D	44.2	34.1	26.6	-	8.1	-
	PreTrimNet [56]	I3D	41.4	32.1	23.1	14.2	7.7	23.7
Weak	UntrimmedNets [43]	-	28.2	21.1	13.7	-	-	-
	Hide-and-seeek [40]	-	19.5	12.7	6.8	-	-	-
	STPN [34]	UNT	31.1	23.5	16.2	9.8	5.1	17.1
	AutoLoc [39]	UNT	35.8	29.0	21.2	13.4	5.8	21.0
	W-TALC [36]	UNT	32.0	26.0	18.8	-	6.2	-
	Liu <i>et al.</i> [26]	UNT	37.5	29.1	19.9	12.3	6.0	21.0
	CleanNet [51]	UNT	37.0	30.9	23.9	13.9	7.1	22.6
	BaS-Net [21]	UNT	42.8	34.7	25.1	17.1	9.3	25.8
	Ours	UNT	44.0	36.5	27.3	18.8	9.6	27.2
	STPN [34]	I3D	35.5	25.8	16.9	9.9	4.3	18.5
	W-TALC [36]	I3D	40.1	31.1	22.8	-	7.6	-
	MAAN [54]	I3D	41.1	30.6	20.3	12.0	6.9	22.2
	Liu <i>et al.</i> [26]	I3D	41.2	32.1	23.1	15.0	7.0	23.7
	TSM [52]	I3D	39.5	-	24.5	-	7.1	-
	Nguyen <i>et al.</i> [35]	I3D	46.6	37.5	26.8	17.6	10.0	27.7
	BaS-Net [21]	I3D	44.6	36.0	27.0	18.6	10.4	27.3
	RPN [17]	I3D	48.2	37.2	27.9	16.7	8.1	27.6
	Ours	I3D	46.9	39.2	30.7	20.8	12.5	30.0

Table 1 demonstrates the results on THUMOS’14. As shown, our method achieves a new state-of-the-art performance on weakly-supervised temporal action localization, regardless of the choice of the feature extractor (UntrimmedNets and I3D). Notably, our method with I3D features significantly outperforms the existing background modeling approaches, Liu *et al.* [26], Nguyen *et al.* [35] and BaS-Net [21], by large margins of 7.6 %, 3.9 % and 3.7 % at the IoU threshold of 0.5, respectively. Moreover, even with a much lower level of supervision, our method performs better than several fully-supervised methods, following the latest fully-supervised approaches with the least gap. The quantitative results on ActivityNet 1.2 are demonstrated in Table 2. Consistent with the results on THUMOS’14, our method outperforms all weakly-supervised approaches. Moreover, our method follows SSN [57] with a small gap, which shows the potential of weakly-supervised action localization. We also summarize the performances on ActivityNet 1.3 in Table 3. We see that our method surpasses all existing weakly-supervised methods including those which use external information.

4.3 Ablation study

We conduct ablation study on THUMOS’14 to investigate the contribution of each component. Firstly, the baseline is set as the main pipeline only with video-level classification loss (\mathcal{L}_{cls}). Thereafter, the proposed losses for background modeling, *i.e.*, uncertainty modeling loss (\mathcal{L}_{um}) and background entropy loss (\mathcal{L}_{be}), are added subsequently. We note that background entropy loss cannot stand alone, as it is calculated with the pseudo background segments which are selected based on feature magnitudes. The mAP at the IoU threshold 0.5 and the average mAP of the variants are reported in Fig. 3. For comparison with different background modeling methods, we also plot the performance

Table 2: Comparison on ActivityNet 1.2. AVG represents the averaged mAP at the thresholds 0.5:0.05:0.95, while † denotes the use of action frequency information. Our method uses I3D features.

Sup.	Method	mAP@IoU (%)										AVG
		0.5	0.55	0.6	0.65	0.7	0.75	0.8	0.85	0.9	0.95	
Full	SSM [57]	41.3	38.8	35.9	32.9	30.4	27.0	22.2	18.2	13.2	6.1	26.6
Weak†	3C-Net [33]	35.4	-	-	-	22.9	-	-	-	8.5	-	21.1
Weak	UntrimmedNets [43]	7.4	6.1	5.2	4.5	3.9	3.2	2.5	1.8	1.2	0.7	3.6
	AutoLoc [39]	27.3	24.9	22.5	19.9	17.5	15.1	13.0	10.0	6.8	3.3	16.0
	CleanNet [51]	37.1	33.4	29.9	26.7	23.4	20.3	17.2	13.9	9.2	5.0	21.6
	W-TALC [36]	37.0	33.5	30.4	25.7	14.6	12.7	10.0	7.0	4.2	1.5	18.0
	Liu <i>et al.</i> [26]	36.8	-	-	-	-	22.9	-	-	-	5.6	22.4
	TSM [52]	28.3	26.0	23.6	21.2	18.9	17.0	14.0	11.1	7.5	3.5	17.1
	RPN [17]	37.6	-	-	-	-	23.9	-	-	-	5.4	23.3
	BaS-Net [21]	38.5	35.5	32.7	29.8	27.1	24.2	20.7	16.7	11.9	5.6	24.3
	Ours	40.3	36.8	34.3	31.6	28.5	25.1	21.8	17.3	12.7	5.9	25.4

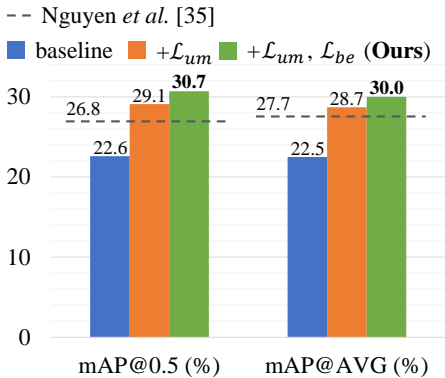


Figure 3: Ablation study on THUMOS'14. The mAP@0.5 and the average mAP under the IoU thresholds 0.3:0.1:0.7 (denoted by AVG) are reported. We also plot the performance of Nguyen *et al.* [35] to compare different background modeling approaches. Full results can be found in the supplementary materials.

Table 3: Comparison on ActivityNet 1.3. AVG means the averaged mAP under the thresholds 0.5:0.05:0.95. † denotes the use of additional information. We note that all methods employ I3D as the feature extractor.

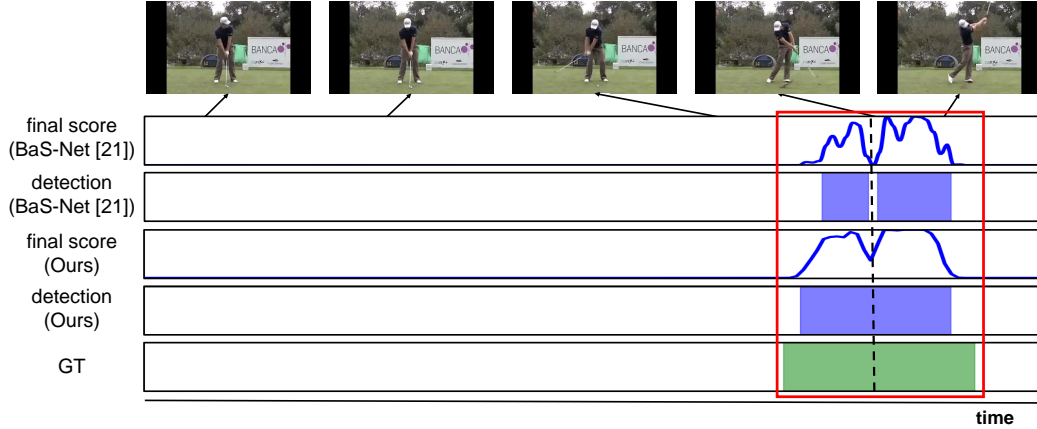
Supervision	Method	mAP@IoU (%)			
		0.5	0.75	0.95	AVG
Full	CDC [38]	45.3	26.0	0.2	23.8
	R-C3D [47]	26.8	-	-	12.7
	TAL-Net [9]	38.2	18.3	1.3	20.2
	BSN [24]	46.5	30.0	8.0	30.0
	GTAN [27]	52.6	34.1	8.9	34.3
	BMN [25]	50.1	34.8	8.3	33.9
P-GCN [55]	48.3	33.2	3.3	31.1	
Weak†	STAR [49]	31.1	18.8	4.7	-
	PreTrimNet [56]	34.8	20.9	5.3	22.5
Weak	STPN [34]	29.3	16.9	2.6	-
	MAAN [54]	33.7	21.9	5.5	-
	Liu <i>et al.</i> [26]	34.0	20.9	5.7	21.2
	TSM [52]	30.3	19.0	4.5	-
	Nguyen <i>et al.</i> [35]	36.4	19.2	2.9	-
	BaS-Net [21]	34.5	22.5	4.9	22.2
Ours	37.0	23.9	5.7	23.7	

of Nguyen *et al.* [35], which pushes background frames into an auxiliary class. As can be seen, we enjoy a large performance gain of 6.5 % in mAP@0.5 by modeling uncertainty with feature magnitudes. Notably, it (+ \mathcal{L}_{um}) outperforms the current state-of-the-art background modeling method by a considerable gap, which verifies the effectiveness of our uncertainty modeling. Moreover, by adding background entropy loss, the performance is further improved, achieving a new state-of-the-art with a large margin.

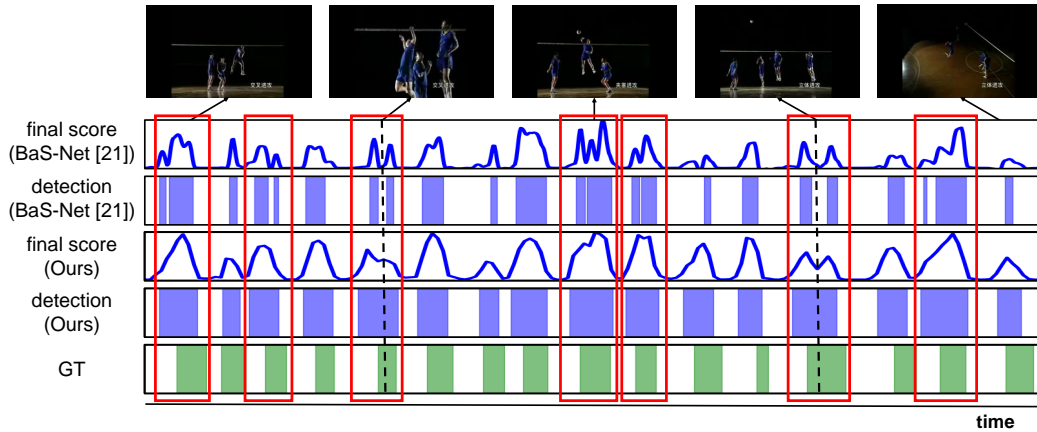
4.4 Qualitative comparison

To confirm the superiority of our background modeling, we compare our method with another background modeling approach by visualization. We choose BaS-Net [21] for comparison, since it is an existing state-of-the-art background modeling method and the implementation is publicly available⁴. As shown in Fig. 4, our model detects the action instances more precisely than BaS-Net. More specifically, in the red boxes, we notice that BaS-Net splits one action instance into multiple incomplete detection results. We conjecture that this problem arises because BaS-Net strongly forces all background frames to belong to a specific class, which makes the model misclassify confusing parts of action instances as the background class and fail to cover complete action instances. On the contrary, our model provides better separation between action and background via uncertainty

⁴<https://github.com/Pilhyeon/BaSNet-pytorch>



(a) An example of *GolfSwing* action



(b) An example of *VolleyballSpiking* action

Figure 4: Qualitative comparison with BaS-Net [21] on THUMOS’14. For each example video, there are five plots with sampled frames. The first and second plot show the final scores and the detection results of the corresponding action class from BaS-Net respectively. The third and fourth plot represent the final scores and the detection results from our model respectively. The last plot denotes the ground truth action intervals. The horizontal axis in each plot means the timesteps of the videos, while the vertical axes of the first and third plots indicates the scores, ranging from 0 to 1. In the red boxes, while BaS-Net fails to cover complete action instances and splits them into multiple detection results, our method is able to accurately localize them.

modeling, which allows our model to successfully localize the complete action instances without false alarms.

5 Conclusion

In this work, we identified the inherent limitations of existing background modeling approaches, with the observation that background frames may be dynamic and inconsistent. Thereafter, based on the properties, we proposed to formulate background frames as out-of-distribution samples and model uncertainty with feature magnitudes. In order to train the model without frame-level annotations, we designed a new architecture, where uncertainty is learned via multiple instance learning. Furthermore, background entropy loss was introduced to prevent background segments from leaning toward any specific action class. Ablation study verified that our uncertainty modeling with feature magnitudes and background entropy loss both are beneficial for the localization performance. Through the extensive experiments on the most popular benchmarks - THUMOS’14 and ActivityNet, our method achieved a new state-of-the-art with a large margin on weakly-supervised temporal action localization.

Broader Impact

Our highly accurate weakly supervised action localization method makes various action detection applications available without intensive manual labeling efforts, which saves a lot of costs. Action detection is widely used in various domains, such as security, education, sports, and entertainment. By exploiting our method, lots of people or organizations can benefit from it, including governments, colleges, movie makers, and even citizens. For example, a possible application is video surveillance for automatic identification of events of interest, *e.g.*, traffic accidents. If the system fails to detect such actions, it may affect some work of traffic police, but it can still reduce their work for detection. Moreover, our method can be used to summarize large-scale online videos with the detected representative actions, which will significantly reduce the human efforts.

References

- [1] H. Alwassel, F. Caba Heilbron, and B. Ghanem. Action search: Spotting actions in videos and its application to temporal action localization. In *ECCV*, pages 251–266, 2018.
- [2] S. Andrews, I. Tsochantaridis, and T. Hofmann. Support vector machines for multiple-instance learning. In *NIPS*, 2002.
- [3] A. Bendale and T. Boulton. Towards open world recognition. In *CVPR*, pages 1893–1902, 2015.
- [4] A. Bendale and T. E. Boulton. Towards open set deep networks. In *CVPR*, pages 1563–1572, 2016.
- [5] P. Bojanowski, R. Lajugie, F. Bach, I. Laptev, J. Ponce, C. Schmid, and J. Sivic. Weakly supervised action labeling in videos under ordering constraints. In *ECCV*, pages 628–643, 2014.
- [6] F. Caba Heilbron, V. Escorcia, B. Ghanem, and J. Carlos Niebles. Activitynet: A large-scale video benchmark for human activity understanding. In *CVPR*, pages 961–970, 2015.
- [7] J. Carreira and A. Zisserman. Quo vadis, action recognition? a new model and the kinetics dataset. In *CVPR*, pages 6299–6308, 2017.
- [8] R. Chalapathy and S. Chawla. Deep learning for anomaly detection: A survey. *arXiv preprint arXiv:1901.03407*, 2019.
- [9] Y.-W. Chao, S. Vijayanarasimhan, B. Seybold, D. A. Ross, J. Deng, and R. Sukthankar. Rethinking the faster r-cnn architecture for temporal action localization. In *CVPR*, pages 1130–1139, 2018.
- [10] J. Deng, W. Dong, R. Socher, L.-J. Li, K. Li, and L. Fei-Fei. Imagenet: A large-scale hierarchical image database. In *CVPR*, pages 248–255, 2009.
- [11] A. R. Dhamija, M. Günther, and T. E. Boulton. Reducing network agnostophobia. In *NeurIPS*, 2018.
- [12] Y. Gal and Z. Ghahramani. Dropout as a bayesian approximation: Representing model uncertainty in deep learning. In *ICML*, pages 1050–1059, 2016.
- [13] Y. Geifman and R. El-Yaniv. Selective classification for deep neural networks. In *NIPS*, pages 4878–4887, 2017.
- [14] A. Graves. Practical variational inference for neural networks. In *NIPS*, pages 2348–2356, 2011.
- [15] D. Hendrycks and K. Gimpel. A baseline for detecting misclassified and out-of-distribution examples in neural networks. In *ICLR*, 2017.
- [16] D.-A. Huang, L. Fei-Fei, and J. C. Niebles. Connectionist temporal modeling for weakly supervised action labeling. In *ECCV*, pages 137–153, 2016.
- [17] L. Huang, Y. Huang, W. Ouyang, and L. Wang. Relational prototypical network for weakly supervised temporal action localization. In *AAAI*, 2020.

- [18] Y.-G. Jiang, J. Liu, A. Roshan Zamir, G. Toderici, I. Laptev, M. Shah, and R. Sukthankar. THUMOS challenge: Action recognition with a large number of classes. <http://csrcv.ucf.edu/THUMOS14/>, 2014.
- [19] H. Kuehne, A. Richard, and J. Gall. Weakly supervised learning of actions from transcripts. *Computer Vision and Image Understanding*, 163:78–89, 2017.
- [20] B. Lakshminarayanan, A. Pritzel, and C. Blundell. Simple and scalable predictive uncertainty estimation using deep ensembles. In *NIPS*, pages 6402–6413, 2017.
- [21] P. Lee, Y. Uh, and H. Byun. Background suppression network for weakly-supervised temporal action localization. In *AAAI*, 2020.
- [22] Y. J. Lee, J. Ghosh, and K. Grauman. Discovering important people and objects for egocentric video summarization. In *CVPR*, pages 1346–1353, 2012.
- [23] S. Liang, Y. Li, and R. Srikant. Enhancing the reliability of out-of-distribution image detection in neural networks. In *ICLR*, 2018.
- [24] T. Lin, X. Zhao, H. Su, C. Wang, and M. Yang. Bsn: Boundary sensitive network for temporal action proposal generation. In *ECCV*, pages 3–19, 2018.
- [25] T. Lin, X. Liu, X. Li, E. Ding, and S. Wen. Bmn: Boundary-matching network for temporal action proposal generation. In *ICCV*, pages 3888–3897, 2019.
- [26] D. Liu, T. Jiang, and Y. Wang. Completeness modeling and context separation for weakly supervised temporal action localization. In *CVPR*, pages 1298–1307, 2019.
- [27] F. Long, T. Yao, Z. Qiu, X. Tian, J. Luo, and T. Mei. Gaussian temporal awareness networks for action localization. In *CVPR*, pages 344–353, 2019.
- [28] Y.-F. Ma, X.-S. Hua, L. Lu, and H.-J. Zhang. A generic framework of user attention model and its application in video summarization. *IEEE Transactions on Multimedia*, 7:907–919, 2005.
- [29] A. Malinin and M. Gales. Predictive uncertainty estimation via prior networks. In *NeurIPS*, pages 7047–7058, 2018.
- [30] A. Malinin and M. Gales. Reverse kl-divergence training of prior networks: Improved uncertainty and adversarial robustness. In *NeurIPS*, pages 14520–14531, 2019.
- [31] A. Malinin, B. Mlodozienec, and M. J. F. Gales. Ensemble distribution distillation. In *ICLR*, 2019.
- [32] O. Maron and T. Lozano-Pérez. Multiple-instance a framework for multiple-instance learning. In *NIPS*, 1998.
- [33] S. Narayan, H. Cholakkal, F. S. Khan, and L. Shao. 3c-net: Category count and center loss for weakly-supervised action localization. In *ICCV*, pages 8678–8686, 2019.
- [34] P. Nguyen, T. Liu, G. Prasad, and B. Han. Weakly supervised action localization by sparse temporal pooling network. In *CVPR*, pages 6752–6761, 2018.
- [35] P. X. Nguyen, D. Ramanan, and C. C. Fowlkes. Weakly-supervised action localization with background modeling. In *ICCV*, pages 5501–5510, 2019.
- [36] S. Paul, S. Roy, and A. K. Roy-Chowdhury. W-talc: Weakly-supervised temporal activity localization and classification. In *ECCV*, pages 563–579, 2018.
- [37] Z. Shou, D. Wang, and S.-F. Chang. Temporal action localization in untrimmed videos via multi-stage cnns. In *CVPR*, pages 1049–1058, 2016.
- [38] Z. Shou, J. Chan, A. Zareian, K. Miyazawa, and S.-F. Chang. Cdc: Convolutional-deconvolutional networks for precise temporal action localization in untrimmed videos. In *CVPR*, pages 5734–5743, 2017.

- [39] Z. Shou, H. Gao, L. Zhang, K. Miyazawa, and S.-F. Chang. Autoloc: Weakly-supervised temporal action localization in untrimmed videos. In *ECCV*, pages 154–171, 2018.
- [40] K. K. Singh and Y. J. Lee. Hide-and-seek: Forcing a network to be meticulous for weakly-supervised object and action localization. In *ICCV*, pages 3544–3553, 2017.
- [41] J. T. Springenberg, A. Klein, S. Falkner, and F. Hutter. Bayesian optimization with robust bayesian neural networks. In *NIPS*, pages 4134–4142, 2016.
- [42] S. Vishwakarma and A. Agrawal. A survey on activity recognition and behavior understanding in video surveillance. *The Visual Computer*, 29:983–1009, 2012.
- [43] L. Wang, Y. Xiong, D. Lin, and L. Van Gool. Untrimmednets for weakly supervised action recognition and detection. In *CVPR*, pages 4325–4334, 2017.
- [44] A. Wedel, T. Pock, C. Zach, H. Bischof, and D. Cremers. An improved algorithm for tv-l 1 optical flow. In *Statistical and geometrical approaches to visual motion analysis*, pages 23–45. Springer, 2009.
- [45] B. Xiong, Y. Kalantidis, D. Ghadiyaram, and K. Grauman. Less is more: Learning highlight detection from video duration. In *CVPR*, pages 1258–1267, 2019.
- [46] Y. Xiong, Y. Zhao, L. Wang, D. Lin, and X. Tang. A pursuit of temporal accuracy in general activity detection. *arXiv preprint arXiv:1703.02716*, 2017.
- [47] H. Xu, A. Das, and K. Saenko. R-c3d: Region convolutional 3d network for temporal activity detection. In *ICCV*, pages 5783–5792, 2017.
- [48] L. Xu, J. S. Ren, C. Liu, and J. Jia. Deep convolutional neural network for image deconvolution. In *NIPS*, pages 1790–1798, 2014.
- [49] Y. Xu, C. Zhang, Z. Cheng, J. Xie, Y. Niu, S. Pu, and F. Wu. Segregated temporal assembly recurrent networks for weakly supervised multiple action detection. In *AAAI*, 2019.
- [50] K. Yang, P. Qiao, D. Li, S. Lv, and Y. Dou. Exploring temporal preservation networks for precise temporal action localization. In *AAAI*, 2018.
- [51] Z. yi Liu, L. Wang, Q. Zhang, Z. Gao, Z. Niu, N. Zheng, and G. Hua. Weakly supervised temporal action localization through contrast based evaluation networks. In *ICCV*, pages 3898–3907, 2019.
- [52] T. Yu, Z. Ren, Y. Li, E. Yan, N. Xu, and J. Yuan. Temporal structure mining for weakly supervised action detection. In *ICCV*, pages 5521–5530, 2019.
- [53] J. Yuan, B. Ni, X. Yang, and A. A. Kassim. Temporal action localization with pyramid of score distribution features. In *CVPR*, pages 3093–3102, 2016.
- [54] Y. Yuan, Y. Lyu, X. Shen, I. W.-H. Tsang, and D.-Y. Yeung. Marginalized average attentional network for weakly-supervised learning. In *ICLR*, 2019.
- [55] R. Zeng, W. Huang, M. Tan, Y. Rong, P. Zhao, J. Huang, and C. Gan. Graph convolutional networks for temporal action localization. In *ICCV*, pages 7093–7102, 2019.
- [56] X. Zhang, H. Shi, C. Li, and P. Li. Multi-instance multi-label action recognition and localization based on spatio-temporal pre-trimming for untrimmed videos. In *AAAI*, 2020.
- [57] Y. Zhao, Y. Xiong, L. Wang, Z. Wu, X. Tang, and D. Lin. Temporal action detection with structured segment networks. In *ICCV*, pages 2914–2923, 2017.
- [58] Z.-H. Zhou. Multi-instance learning: A survey. *Department of Computer Science & Technology, Nanjing University, Tech. Rep*, 2004.